ResearchGate

See discussions, stats, and author profiles for this publication at: https://www.researchgate.net/publication/249609270

# An Illustrative Model of Seasonal and Interannual Variations of the Stratospheric Circulation

**Article** *in* Journal of the Atmospheric Sciences · August 1990

DOI: 10.1175/1520-0469(1990)047<1845:AIMOSA>2.0.CO;2

CITATIONS
40

READS
9

**1 author:**

Shigeo Yoden
Kyoto University

**137** PUBLICATIONS **2,325** CITATIONS

SEE PROFILE

**Some of the authors of this publication are also working on these related projects:**

Project Atmospheric Dynamics View project

Project Research paper during PhD program in Kyoto University View project

All content following this page was uploaded by Shigeo Yoden on 15 September 2015.

The user has requested enhancement of the downloaded file.

# An Illustrative Model of Seasonal and Interannual Variations of the Stratospheric Circulation

SHIGEO YODEN

*Department of Geophysics, Kyoto University, Kyoto, Japan*

(Manuscript received 26 September 1989, in final form 13 January 1990)

ABSTRACT

A simple wave-zonal flow interaction model, originally developed by Holton and Mass, is used to illustrate a rudimentary conception of seasonal and interannual variations of the stratospheric circulation.

The radiative heating is varied periodically with an annual component to investigate the response of the circulation (i.e., the seasonal variation) to the periodic forcing. The response is qualitatively different depending on the wave forcing from the troposphere. The difference resembles that of the climatological seasonal march between the Northern and the Southern hemispheres.

No example of interannual variations (namely, nonperiodic responses) was obtained for the periodic annual forcing. Interannual variation of external conditions is necessary in the present model to obtain interannual variations. A finite range of year-to-year variations of the wave forcing can produce large interannual variability as in the Northern Hemisphere.

## 1. Introduction

Seasonal variation is the atmospheric response to the annual forcing by solar radiation. There are two remarkable differences of the response in the stratosphere to nearly the same annual radiative forcing:

1) Year-to-year differences; i.e., interannual variations.
2) Differences between the Northern and the Southern hemispheres.

The interannual variability in the stratosphere is large during winter in high latitudes of the Northern Hemisphere. The variable range of monthly mean 30-mb temperature at the North Pole is over 30 K in January, but only 4 K in July (Labitzke 1982). The large variability in January is closely related to whether or not a midwinter stratospheric sudden warming occurs. In contrast the interannual variability is large during spring in the Southern Hemisphere. Shiotani and Hirota (1985) pointed out the interannual variability of the timing of the shift and breakdown of the polar night jet. Time–latitude sections of the interannual variability, assembled by Randel (1987) with the Climate Analysis Center data, show that the above interannual variability in both hemispheres is seen in the zonal mean temperature and the zonal-mean zonal–wind through the stratosphere.

The differences of the climatological seasonal march between the two hemispheres have been pointed out for zonal mean quantities and deviations from the zonal mean (e.g., see Andrews 1989). The polar night jet is much stronger in the Southern Hemisphere than in the Northern Hemisphere. The planetary-wave activity is large during winter in the Northern Hemisphere, while it is large after the equinoxes and small in midwinter in the Southern Hemisphere (see Randel 1987).

There are several possible explanations of the interannual variability. Most of them are based on variations of the external (or boundary) conditions. Holton and Tan (1980, 1982) pointed out the influence of the equatorial quasi-biennial oscillation (QBO) on higher latitudes from monthly mean data for a 16-year period. Variations in the position of the zero mean wind critical line and the meridional profile of the mean zonal wind associated with the equatorial QBO may influence the planetary waves (and the mean zonal wind) in the extratropics. These are variations of the "side boundary" of the extratropics in the stratosphere.

Another possibility is the influence of the tropospheric variations such as the El Niño/Southern Oscillation (ENSO) (Labitzke 1982; Wallace and Chang 1982; van Loon and Labitzke 1987). Interannual variations in the troposphere may influence the stratosphere. The variation of planetary waves in the troposphere means the variation of wave forcing at the "bottom boundary" of the stratosphere. In addition, variation of the intensity of the Hadley circulation may cause variation of subtropical jet.

*Corresponding author address:* Dr. Shigeo Yoden, Department of Geophysics, Kyoto University, Kyoto, 606, Japan.

© 1990 American Meteorological Society

Variations of solar activity may influence the stratosphere through radiative heating. The 11-year solar cycle is the most significant component of the variations with a period longer than a year. The direct radiative effect is estimated to be very small in the stratosphere, but there is apparently a significant correlation between the solar cycle and the stratospheric temperature and geopotential height if the data are divided into two groups according to the phase of the equatorial QBO (Labitzke and van Loon 1988; Labitzke and Chanin 1988). At present there is no explanation for the apparent association between the solar cycle, the QBO, and the atmosphere.

Other explanations for interannual variability are based on variations due to nonlinear internal dynamics. Yoden (1987a, hereafter referred to as Y87a) pointed out the possibility of multiple stable states in winter using a simple wave-zonal flow interaction model. Two stable states, one of which is close to the radiative equilibrium and the other is the "stratospheric vacillation" (i.e., periodic occurrence of stratospheric sudden warmings), can exist under the same external conditions. If one of the two states is selected randomly in each winter, there exists interannual variability even under the same external conditions.

There are not enough observations to support or to refute these explanations of the interannual variability.

One of the possible causes of the differences in the seasonal variations between the two hemispheres is the elliptic revolution of the earth. However, the direct radiative effect is expected to be small compared with the observed temperature difference. Another more important cause is the planetary-wave forcing from the troposphere. Some mechanistic models of the seasonal cycle in the middle atmosphere show that the seasonal cycles of mean zonal wind and planetary waves are qualitatively different depending on the tropospheric forcing of planetary waves (Holton and Wehrbein 1980, 1981; Plumb 1989).

In this paper a simple wave–zonal flow interaction model is used to illustrate a rudimentary conception of seasonal and interannual variations in both hemispheres. Time-dependent responses of the model to the annual forcing are computed under several different magnitudes of the planetary-wave forcing, aiming at the differences between the two hemispheres. The results are further investigated by comparing them with the steady solutions under perpetual conditions.

## 2. Model

The model is identical to that used in Y87a. It is a highly truncated spectral model in a $\beta$-channel. The mean zonal wind $\bar{u}$ and the geostrophic streamfunction $\psi'$ are assumed as follows:

$$\bar{u}(y, z, t) = U(z, t) \sin ly, \tag{1}$$

$$\psi'(x, y, z, t) = \mathrm{Re}[\Psi(z, t)e^{ikx}]e^{z/2H} \sin ly . \tag{2}$$

The dependent variables $U(z, t)$ and $\Psi(z, t)$ are governed by the zonal mean and the wave part of quasi-geostrophic potential vorticity equations, respectively; their schematic description is

$$\frac{\partial U}{\partial t} = \mathcal{F}\left(U, \Psi; \frac{dU_R}{dz}\right), \tag{3}$$

$$\frac{\partial \Psi}{\partial t} = \mathcal{G}(U, \Psi; h_B). \tag{4}$$

Two important parameters in this study are mean zonal wind in radiative equilibrium $U_R(z, t)$ and wave amplitude at the bottom boundary $h_B(t) = \Psi(0, t)f_0/g$, where $f_0$ is the Coriolis parameter and $g$ the gravitational acceleration. For simplicity $dU_R/dz$ is assumed to be constant with height throughout this study: $U_R(z, t) = U_{RB} + \Lambda(t) \times z$, where $U_{RB}$ is fixed at 10 m s$^{-1}$. This assumption is equivalent to a constant meridional differential heating with height from the thermal wind relation. The wave forcing $h_B$ is assumed to be constant with time for most cases in this study. Other parameters are identical to those in Y87a.

This is a forced-dissipative system with nonlinear interaction. The system is forced by the differential heating in the zonal component ($dU_R/dz$) and by the wave forcing at the bottom ($h_B$). It is dissipated by Newtonian damping in the wave component. The Newtonian heating/cooling coefficient $\alpha$ is given by $\alpha(z) = \{1.5 + \tanh[(z - 25/7]\} \times 10^{-6}$ s$^{-1}$, where $z$ is given in kilometers. The nonlinear wave-zonal flow interactions are the acceleration of zonal flow due to divergence of the EP flux in $\mathcal{F}$ and the changes in the characteristics of upward wave propagation due to mean zonal flow changes in $\mathcal{G}$.

Equations (3) and (4) are transformed into a set of ordinary differential equations by finite differencing in vertical. This set is not an autonomous system because the external parameters depend on time.

## 3. Results

### a. Steady solutions in a parameter space

Both stable and unstable steady solutions are obtained in a two-dimensional parameter space $h_B - dU_R/dz$ with the same method as in Y87a. The two parameters are set to be constant with time (namely, under perpetual conditions) with ranges of $0 \text{ m} \leqslant h_B \leqslant 250$ m, and $-2.0 \times 10^{-3}$ s$^{-1} \leqslant dU_R/dz \leqslant 3.2 \times 10^{-3}$ s$^{-1}$. Figure 1 shows number of steady solutions obtained numerically in the two-dimensional parameter space. There are multiple steady solutions in the shaded area; i.e., for a pair of values ($h_B$, $dU_R/dz$) lying within the shaded area, we obtained more than one steady solution (three steady solutions). Outside the shaded area, on the other hand, we obtained only one steady solution for a pair of ($h_B$, $dU_R/dz$).

Vertical profiles of the mean zonal wind of the steady

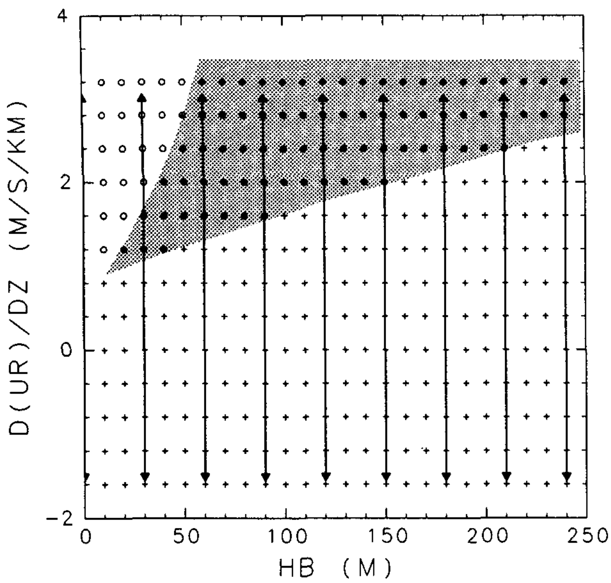


FIG. 1. Number of steady solutions in a two-dimensional parameter space $dU_R/dz$ (ordinate) and $h_B$ (abscissa): Three steady solutions are obtained in the shaded area, and one solution outside the shade. The region denoted by plus signs corresponds to the "lower" leaf of the "cusp surface" of steady solutions shown in Fig. 3, and that by the circles corresponds to the "upper" leaf.

solutions are shown in Fig. 2 for $h_B = 90$ m and several values of $dU_R/dz$ (see also Fig. 2 in Y87a). Three steady solutions are obtained for $dU_R/dz \geqslant 1.6 \times 10^{-3}$ $s^{-1}$; the steady solutions denoted by solid lines have a large reduction of mean zonal wind due to the dissipation of upward propagating wave, those denoted by dashed lines are close to the radiative equilibrium with little wave propagation, and those denoted by dotted lines are intermediate between above two groups. Details of the dynamics of these steady solutions are given by Yoden (1987b).

The set of steady solutions constitutes a "cusp surface" in a three-dimensional phase space [the two external parameters plus one dependent variable, say, $U$ ($z = 35$ km)]. Three-dimensional perspectives of the cusp surface are shown in Figs. 3a,b from two different viewpoints. The three leaves of the solution are named the "upper," "middle," and "lower" leaf according to the magnitude of the mean zonal wind. The intersection of the leaves and a plane of constant $dU_R/dz$ ($=2 \times 10^{-3}$ $s^{-1}$) is a bifurcation diagram for the parameter $h_B$ (Fig. 3 in Y87a).

A bifurcation diagram for another intersection is shown in Fig. 4 for a plane of constant $h_B$ (= 90 m). For "summer" conditions with negative $dU_R/dz$, only one solution is obtained, which is stable for any perturbation. The "lower" branch is unstable for $dU_R/dz \geqslant 0$ $s^{-1}$. There exists a periodic solution for $dU_R/dz \geqslant 0$ $s^{-1}$, which is the stratospheric vacillation obtained by Holton and Mass (1976). The stable "upper" branch and unstable "middle" branch also exist for "winter" conditions with positively large $dU_R/dz$.

At this point we have some interesting questions:

- What kind of response is obtained if $dU_R/dz$ is changed periodically with time (particularly, with a period of a year)? *If a non-periodic response is obtained for the periodic annual forcing, it is an example of interannual variation caused by the internal dynamics.*
- Does the response for annual forcing depend on the other parameter $h_B$, the wave forcing at the bottom boundary? If yes, how does it depend on the parameter? *These questions are interesting in relation to the differences between the Northern and the Southern hemispheres.*
- How does the response depend on the ratio of the period of forcing and the relaxation time of the Newtonian heating? *From the answer to this we can assess the adequateness of quasi-static arguments for the seasonal variations under perpetual conditions.*

### b. *Time-dependent response to annual forcing*

The radiative heating is changed with an annual component as,

$$\frac{dU_R}{dz}(t) = 0.75 - 2.25 \cos\omega_a t \quad [\times 10^{-3}\ s^{-1}], \qquad (5)$$

where $\omega_a$ is a frequency of annual variation: $\omega_a = 2\pi/365$, and the unit of time $t$ is day. The wave forcing is fixed at $h_B = 0$ m, 30 m, · · ·, or 240 m. The range of annual variation of the parameters is ~~shown in~~ Fig. 1.

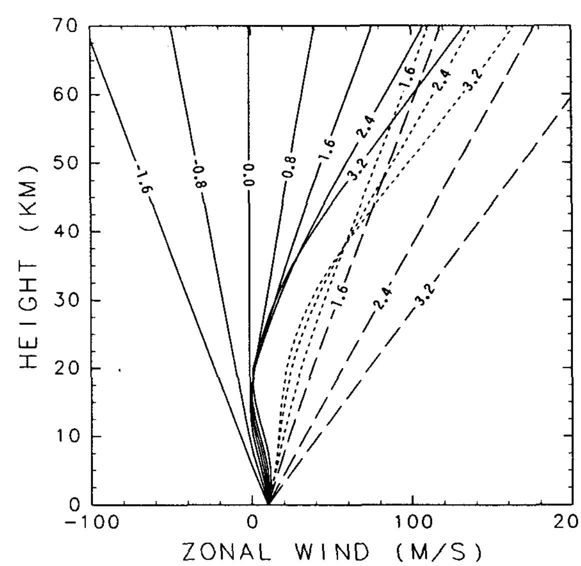


FIG. 2. Vertical profile of mean zonal wind of steady solutions at $h_B = 90$ m. Number on each line is $dU_R/dz$ [$\times 10^{-3}$ $s^{-1}$]. Solid lines denote solutions of the "lower" leaf, dotted lines the "middle" leaf, and dashed lines the "upper" leaf.

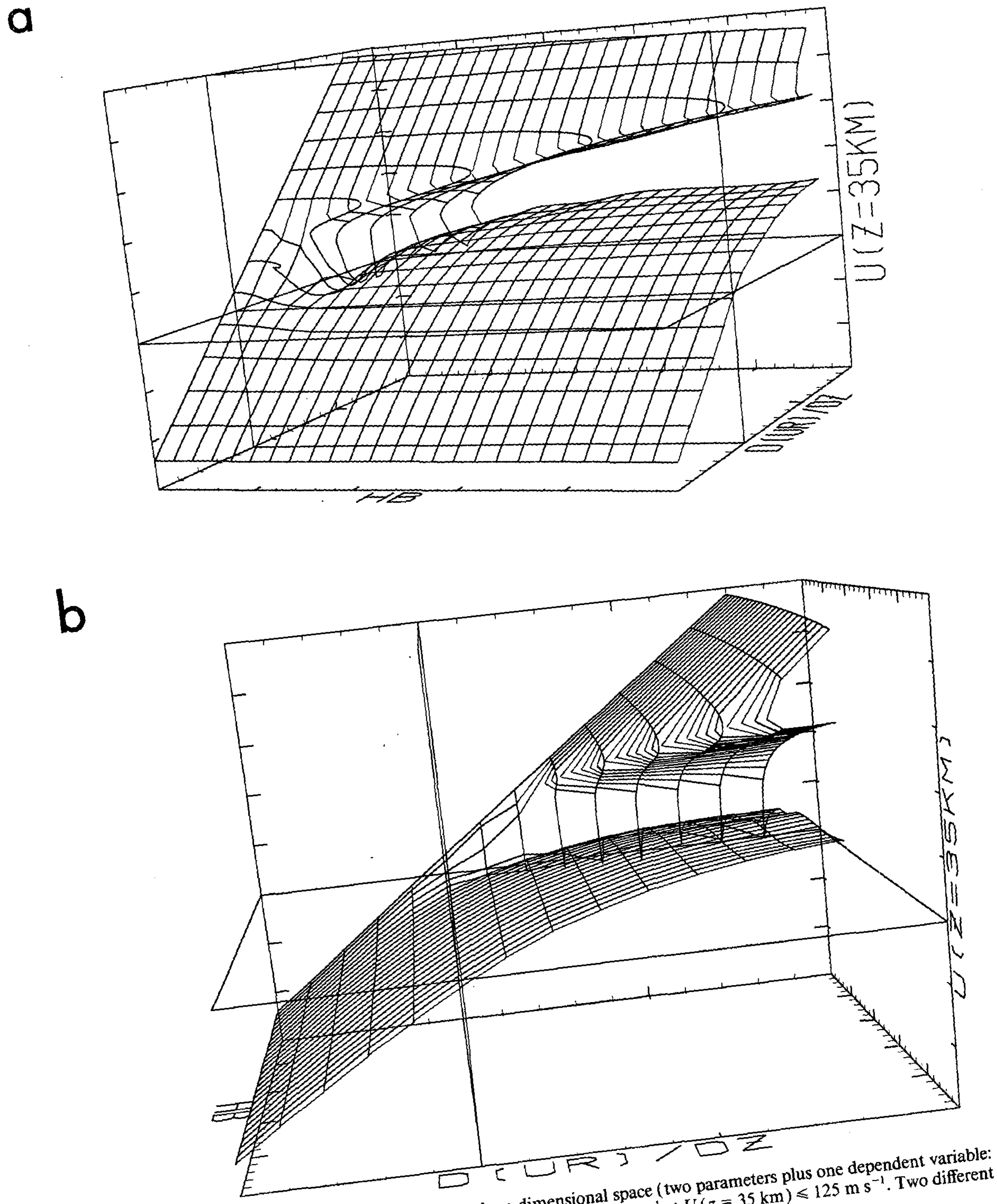


FIG. 3. Cusp surface of steady solutions in a three-dimensional space (two parameters plus one dependent variable: $0 \text{ m} \leq h_B \leq 250 \text{ m}$, $-2 \times 10^{-3} \text{ s}^{-1} \leq dU_R/dz \leq 4 \times 10^{-3} \text{ s}^{-1}$, $-75 \text{ m s}^{-1} \leq U(z = 35 \text{ km}) \leq 125 \text{ m s}^{-1}$. Two different perspectives are shown in (a) and (b).

We obtained only a periodic response to the annual forcing of the radiative heating for the nine cases of $h_B$. Figure 5 shows the periodic variation of mean zonal wind $U$ at the 35 km level with the variation of radiatively equilibrated $U_R(z = 35 \text{ km}, t)$. The mean zonal wind is close to the "radiative equilibrium" wind with

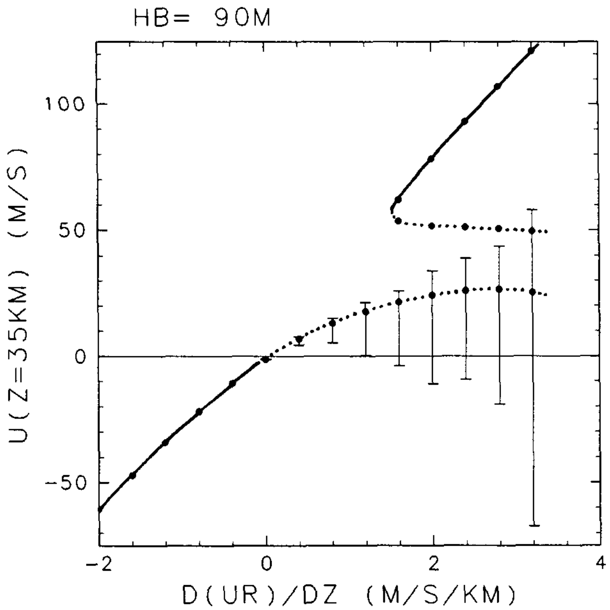


FIG. 4. Bifurcation diagram for the external parameter $dU_R/dz$ ($h_B$ = 90 m). Mean zonal wind at the 35 km level is plotted. Stable steady solutions are denoted by a solid line and unstable ones by a dotted line. A vertical bar is the range of stable periodic solution obtained by a time integration.

a lag for small values of $h_B$. For $h_B$ = 30 m there are depressions after the equinoxes. The mean zonal wind is largely reduced from the "radiative equilibrium" wind in winter for $h_B \geq 60$ m because of the dissipation of propagating Rossby waves. We observe "minor," "major" and "final" sudden warmings in Fig. 5b.

In order to understand the response deeply, the periodic solutions are drawn onto the bifurcation diagrams as shown in Figs. 6a–d. For $h_B$ = 0 m, the periodic trajectory is elliptic in the $dU_R/dz - U(z = 35$ km) plane. When $\Psi = 0$, Eq. (3) is simplified if we assume that $l \rightarrow 0$ and the Newtonian heating/cooling coefficient is constant with height, $\alpha_0$:

$$\frac{\partial U}{\partial t} + \alpha_0 U = \alpha_0 U_R(t) + C,$$

$$= A \cos\omega_a t + C', \qquad (6)$$

where $A$, $C$ and $C'$ are constants. A general solution is

$$U = U_0 e^{-\alpha_0 t} + \frac{A}{\sqrt{\alpha_0^2 + \omega_a^2}} \cos(\omega_a t - \delta) + \frac{C'}{\alpha_0}, \qquad (7)$$

where $\delta = \arctan(\omega_a/\alpha_0)$. It is a periodic response with a lag $\delta$, because the first term on the rhs decays out with time. If the relaxation time of the radiative heating is much smaller than a year ($\alpha_0 \gg \omega_a$), $\delta \sim 0$, namely, there is no lag between the forcing and the response. Therefore the trajectory of the periodic response is on the line of steady solutions in Fig. 6a. Quasi-static arguments are all right for this limit. Because $\alpha^{-1} \sim O(1 \sim 10$ days) and $\omega_a^{-1} \sim 58$ days in this study, the response has a finite lag from the forcing. Therefore the trajectory is elliptic in Fig. 6a.

For a small value of the wave forcing ($h_B$ = 30 m), two limit points of steady solutions exist within the annual range of $dU_R/dz$, which are denoted by **X**s in

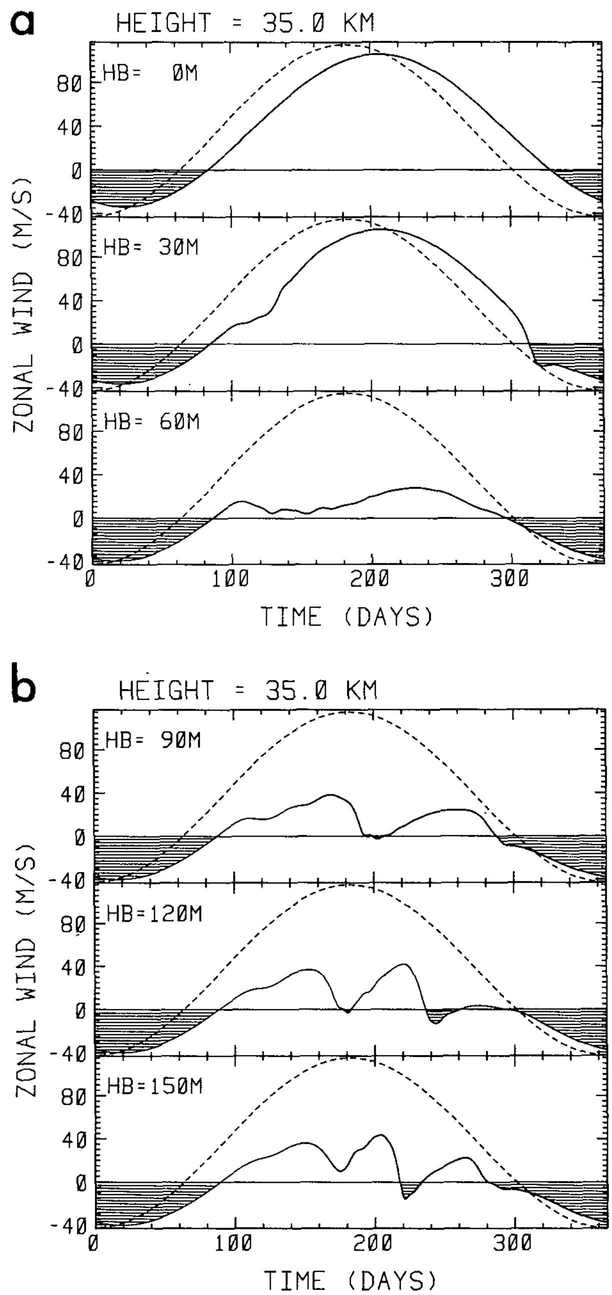


FIG. 5. Periodic response to the annual forcing of the radiative heating for (a), $h_B$ = 0 m, 30 m, 60 m, and (b) 90 m, 120 m, 150 m. Solid line denotes the periodic variation of mean zonal wind $U$ at the 35 km, and dotted line denotes the annual variation of radiatively equilibrated $U_R(t)$ at the same level. Periods of easterly wind are shaded.

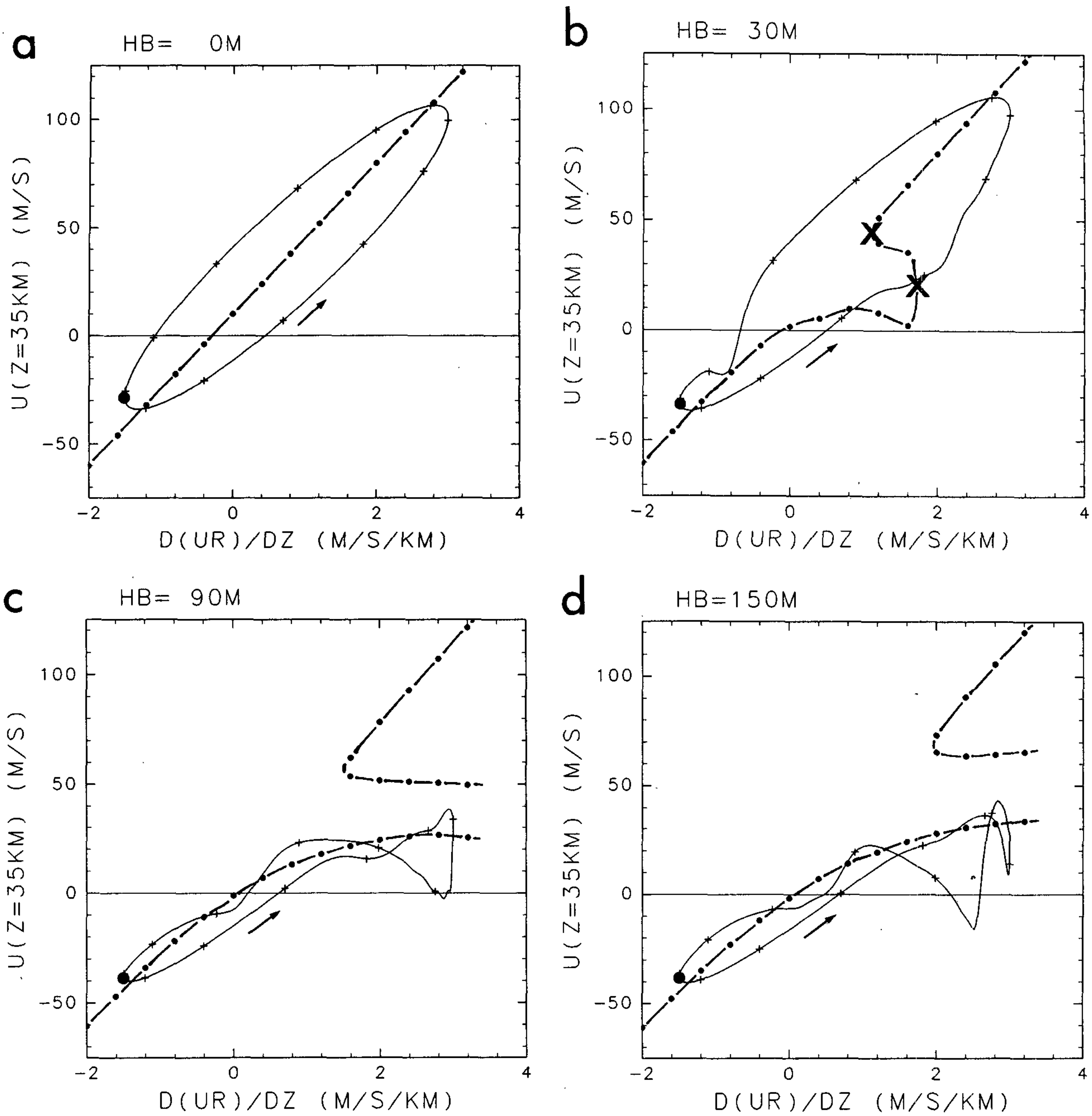


FIG. 6. Periodic solutions to the annual forcing projected onto $dU_R/dz - U(z = 35\text{ km})$ plane: (a) $h_B = 0$ m, (b) $h_B = 30$ m, (c) $h_B = 90$ m, and (d) $h_B = 150$ m. "Summer solstice" is denoted by a large dot and plus signs are marked every 30 days after the dot. Steady solution branches under perpetual external conditions are also drawn by dash-dotted lines.

Fig. 6b. If we assume a quasi-static variation of $dU_R/dz$, transitions take place at the limit points, one of which is a "catastrophic sudden warming" after midwinter from the "upper" leaf to the "lower" leaf discussed by Chao (1985) (see also Fig. 8 in Y87a). The response is not quasi-static at the present value of $\alpha$; however, there still remains the vestige of transitions. The vestige corresponds to the depressions after the equinoxes in Fig. 5.

For larger values of wave forcing ($h_B > 50$ m), on the other hand, one of the limit points is outside of the annual range of $dU_R/dz$. As a result, there is no transition in the annual variation. The "lower" leaf, namely the vacillation branch, is selected every winter [Figs. 6c,d]. The stable state of the "upper" leaf is not realized under the present external conditions.

Time-height sections of $U(z, t)$ and $|\Psi(z, t)|$ are shown in Fig. 7 for $h_B = 30$ m. The wave amplitude has large values after the equinoxes. These periods correspond to those of transitions in Fig. 6b. In midwinter, the mean zonal wind is very large, while the wave amplitude is small. The seasonal behavior is qualitatively different for $h_B$ = 90 m as shown in Fig. 8. The wave amplitude has large values in midwinter. The mean zonal wind in winter is small compared with that for small $h_B$ because "midwinter" and "final" sudden warmings take place.

## 4. Discussion

The questions raised at the end of section 3.1 are generalized as a problem about the response of nonlinear nonautonomous systems to periodic variations of external forcing. The key parameters are amplitude and frequency of the forcing, and relaxation time of the system. A nonperiodic solution is *not* obtained for the annual forcing; the small ratio of $\omega_a/\alpha$ ($\sim$0.4 at $z$ = 0 km, and $\sim$0.083 at $z$ = 35 km) is an important factor for this reason. In the limit of $\alpha \rightarrow \infty$ the response is quasi-static and therefore periodic.

On the other hand, nonperiodic responses are obtained in another series of numerical experiments in which the frequency of forcing is the same order as $\alpha$. In these experiments only the wave forcing was changed periodically;

$$h_B(t) = 130 + 30 \cos\omega_i t \quad [\mathrm{m}], \tag{8}$$

with $dU_R/dz = 2 \times 10^{-3}$ s$^{-1}$, in order to gain some understanding of the response to the intraseasonal variations of wave forcing from the troposphere. Nonperiodic solutions are obtained for 0.0459 day$^{-1} \leq \omega_i \leq$ 0.0823 day$^{-1}$ (i.e., the period of the forcing is from 21.8 days to 12.2 days). These values are comparable to those of the relaxation time near the bottom boundary, 23.1 days at $z$ = 0 km and 11.6 days at $z$ = 25 km. The period of the vacillation under a perpetual forcing condition may be another important time scale for the nonperiodicity, which is 90.9 days for $h_B$ = 100 m, and 39.9 days for $h_B$ = 160 m.

From these numerical experiments it is conjectured that there is not likely to exist interannual variability due to internal dynamics in the extratropical stratosphere under purely periodic annual forcing. This is primarily due to the smallness of the heat capacity in the stratosphere. In the troposphere, on the other hand, the relaxation time is much longer than in the stratosphere, because the troposphere is directly linked to the ocean and the ice, which have large heat capacity. Therefore it is expected that interannual variations may be caused more easily in the troposphere even under purely periodic solar forcing. In other words, there is no memory with time scales longer than a year in the stratosphere; time evolution in a previous winter is cleared in the next summer.

Interannual variations of the external (or boundary) conditions cause interannual variability in the stratosphere. The present model can produce the two differences of stratospheric circulation stated in the Introduction, if the wave forcing at the bottom has a variation. When the wave forcing is different in each winter with a finite range, it can produce large interannual variability that contains the occurrence of sudden warmings. Furthermore, it can produce a qualitatively different type of circulation like that observed in the Southern Hemisphere, if the wave forcing is further reduced. These results have been obtained fragmentarily by time integrations of several mechanistic numerical models with an annual forcing (Holton and Wehrbein 1980, 1981; Wakata and Uryu 1987; Plumb 1989).

It is worthwhile to examine the difference between these numerical studies and the present one. Holton and Wehrbein (1980, 1981) obtained the different seasonal behavior between the two hemispheres for the first time. However, they did not pay much attention to the difference, probably because observations in the Southern Hemisphere were not sufficient in those days. Plumb (1989) was the first to point out the difference. His model is similar to the present model except for the external parameters and the vertical profile of $U_R(z, t)$. Consequently, our results shown in Figs. 7 and 8 are qualitatively similar to those obtained by Plumb (1989). Our originality is the interpretation of the difference in terms of steady and periodic nonlinear solutions in phase space (Figs. 3 and 6). It is revealed

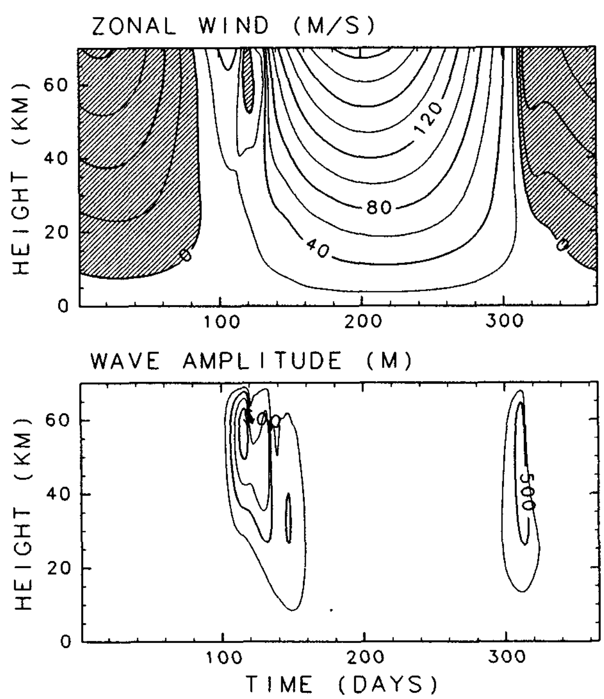


FIG. 7. Time–height sections of the mean zonal wind $U(z, t)$ and the wave amplitude $|\Psi(z, t)|$; $h_B$ = 30 m. Contour intervals are 20 m s$^{-1}$ for the mean zonal wind and 250 m for the wave amplitude.

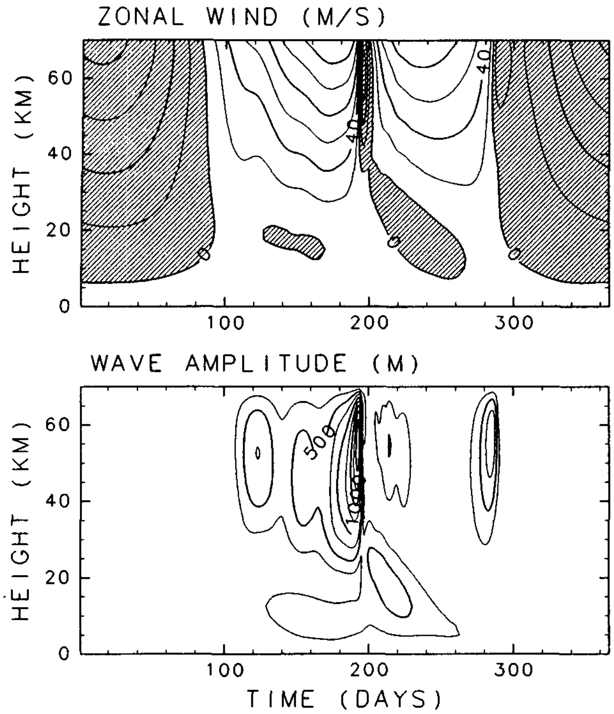


FIG. 8. As in Fig. 7 but for $h_B$ = 90 m.

that Plumb's conjecture upon the difference with linear quasi-static arguments is misleading. Wakata and Uryu (1987) made a similar analysis to ours, but they analyzed only the case of weak wave-forcing, because their model has a different lower boundary condition for the wave.

The present model is too simple to examine the effect of the equatorial QBO. Variations of the critical latitude of Rossby waves due to the QBO could be incorporated into the model by changing the channel width, if the critical line acts as a perfect reflector; however, this is a very crude assumption. Besides, many meridional modes, instead of one mode, are necessary to represent the variation of the meridional profile of the mean zonal wind.

In Y87a three theories of stratospheric sudden warmings are illustrated on a bifurcation diagram (Fig. 8 in Y87a), which is an intersection of three leaves at a constant $dU_R/dz$ in Fig. 3. A transition from the "upper" leaf to the "lower" leaf is a key mechanism in two of the theories. In Matsuno's (1971) theory, impulsive initiation of a wave forcing causes the transition. Chao's (1985) catastrophe theory treats the transition at a limit point under quasi-static variation of wave forcing. The other is the vacillation obtained by Holton and Mass (1976). In the present experiments, only the vacillation branch is selected with the annual variation of radiative forcing, because the vacillation branch bifurcates from the "lower" leaf of steady solutions, around which the summer type of circulation is located (Fig. 4). To realize the transition types of sudden warmings in this model, it is necessary to reach the "upper" leaf in winter. The wave forcing at the bottom must be small enough to make the transition to the "upper" leaf before midwinter. Both numerical and observational studies are necessary with the conceptions obtained here in order to assess the above theories of sudden warmings.

## 5. Conclusion

Time-dependent response of a simple wave-zonal flow interaction model to the annual forcing of radiative heating was investigated to obtain a rudimentary conception of seasonal and interannual variations of the stratospheric circulation. The response is qualitatively different depending on the magnitude of wave forcing at the bottom boundary: For small values of the wave forcing, there are rapid transitions of the zonal mean quantities after the equinoxes. The wave activity is large during the transition periods and has a local minimum in midwinter. On the other hand, there is no transition for large values of the wave forcing. The vacillation branch of a series of sudden warmings is selected every winter as a regular seasonal march. The difference of the response depending on the wave forcing is an explanation of the difference of the seasonal march between the Northern and the Southern hemispheres.

Quasi-static arguments are not very appropriate to understand the dynamics of these seasonal variations because the relaxation time, particularly in the lower stratosphere, is not negligibly small compared with the time scale of the annual forcing.

No example of interannual variations (namely, nonperiodic responses) was obtained for the periodic annual forcing. The reason is the smallness of heat capacity in the stratosphere. Interannual variation of external conditions is necessary in the present model to obtain the interannual variations. A finite range of year-to-year variations of the wave forcing can produce large interannual variability as in the Northern Hemisphere.

The next step is to investigate the seasonal and the interannual variations in more realistic models with the conception obtained in this study. Such an investigation will bring deeper insights with more confidence into the seasonal and the interannual variations of the real stratosphere.

*Acknowledgments.* I wish to thank J. R. Holton, W. A. Robinson, and an anonymous reviewer for their valuable comments. This work was supported in part by Grant-in-Aid for Scientific Reserch from the Ministry of Education.

REFERENCES

Andrews, D. G., 1989: Some comparisons between the middle atmosphere dynamics of the southern and northern hemispheres. *Pure Appl. Geophys.*, **130**, 213–232.

Chao, W. C., 1985: Sudden stratospheric warmings as catastrophes. *J. Atmos. Sci.,* **42,** 1631–1646.

Holton, J. R., and C. Mass, 1976: Stratospheric vacillation cycles. *J. Atmos. Sci.,* **33,** 2218–2225.

——, and H.-C. Tan, 1980: The influence of the equatorial quasi-biennial oscillation on the global circulation at 50 mb. *J. Atmos. Sci.,* **37,** 2200–2208.

——, W. M. Wehrbein, 1980: The role of forced planetary waves in the annual cycle of the zonal mean circulation of the middle atmosphere. *J. Atmos. Sci.,* **37,** 1968–1983.

——, and ——, 1981: A further study of the annual cycle of the zonal mean circulation in the middle atmosphere. *J. Atmos. Sci.,* **38,** 1504–1509.

——, and H.-C. Tan, 1982: The quasi-biennial oscillation in the northern hemisphere lower stratosphere. *J. Meteor. Soc. Jpn.,* **60,** 140–148.

Labitzke, K., 1982: On the interannual variability of the middle stratosphere during the northern winters. *J. Meteor. Soc. Jpn.,* **60,** 124–139.

——, and M. L. Chanin, 1988: Changes in the middle atmosphere in winter related to the 11-year solar cycle. *Ann. Geophys.,* **6,** 643–644.

——, and H. van Loon, 1988: Associations between the 11-year solar cycle, the QBO and the atmosphere. Part I: The troposphere and stratosphere in the northern hemisphere in winter. *J. Atmos. Terr. Phys.,* **50,** 197–206.

Matsuno, T., 1971: A dynamical model of the stratospheric sudden warming. *J. Atmos. Sci.,* **28,** 1479–1494.

Plumb, R. A., 1989: On the seasonal cycle of stratospheric planetary waves. *Pure Appl. Geophys.,* **130,** 233–242.

Randel, W. J., 1987: *Global Atmospheric Circulation Statistics, 1000–1 mb.* NCAR Tech. Note, 295, 245 pp.

Shiotani, M., and I. Hirota, 1985: Planetary wave–mean flow interaction in the stratosphere: A comparison between northern and southern hemispheres. *Quart. J. Roy. Meteor. Soc.,* **111,** 309–334.

van Loon, H., and K. Labitzke, 1987: The southern oscillation. Part V: The anomalies in the lower stratosphere of the northern hemisphere in winter and a comparison with the quasi-biennial oscillation. *Mon. Wea. Rev.,* **115,** 357–369.

Wakata, Y., and M. Uryu, 1987: Stratospheric multiple equilibria and seasonal variations. *J. Meteor. Soc. Jpn.,* **65,** 27–42.

Wallace, J. M., and F.-C. Chang, 1982: Interannual variability of the wintertime polar vortex in the northern hemisphere middle stratosphere. *J. Meteor. Soc. Jpn.,* **60,** 149–155.

Yoden, S., 1987a: Bifurcation properties of a stratospheric vacillation model. *J. Atmos. Sci.,* **44,** 1723–1733.

——, 1987b: Dynamical aspects of stratospheric vacillations in a highly truncated model. *J. Atmos. Sci.,* **44,** 3683–3695.